Dendritic Cell Depletion and Repopulation in the Lung after Irradiation and Bone Marrow Transplantation in Mice

Ines Hahn[1], Anna Klaus[1], Regina Maus[1], John W. Christman[3], Tobias Welte[2], and Ulrich A. Maus[1]

[1]Department of Experimental Pneumology, and [2]Clinic for Pneumology, Hannover School of Medicine, Hannover, Germany; and [3]Department of Pulmonary, Critical Care, and Sleep Medicine, University of Illinois at Chicago, Chicago, Illinois

Dendritic cells (DCs) are essential for innate and adaptive immunity, but are purported to exhibit variable radiosensitivity in response to irradiation in various bone marrow transplantation (BMT) protocols. To address this controversy, we analyzed the magnitude of depletion and repopulation of both lung CD11b^{pos} DC and CD103^{pos} DC subsets in response to irradiation and BMT in a murine model. In our study, CD45.2^{pos} donor bone marrow cells were transplanted into irradiated CD45.1^{pos} recipient mice to examine the depletion of recipient DC subsets and the repopulation of donor DC subsets. We observed an apoptosis-mediated and necrosis-mediated depletion ($>$ 90%) of the recipient CD103^{pos} DC subset, and only a 50–60% depletion of recipient CD11b^{pos} DCs from lung parenchymal tissue on Days 3 and 5, whereas recipient alveolar and lung macrophages were much less radiosensitive, showing an approximately 50% depletion by Days 14–21 after treatment. A repopulation of lung tissue with donor DC subsets had occurred by Days 10 and 28 for CD11b^{pos} DCs and CD103^{pos} DCs, whereas alveolar and lung macrophages were repopulated by 6 and 10 weeks after treatment. Furthermore, the infection of mice with *Streptococcus pneumoniae* further accelerated the turnover of lung DCs and lung macrophage subsets. Our data illustrate the vulnerability of lung CD103^{pos} DCs and CD11b^{pos} DCs to irradiation, and indicate that an accelerated turnover of lung DC subsets occurs, relative to pulmonary and lung macrophages. Our findings may have important implications in the development of adjuvant immune-stimulatory protocols that could reduce the risk of opportunistic infections in patients undergoing BMT.

Keywords: dendritic cell; macrophage; pneumonia; *Streptococcus pneumoniae*; CD103

Dendritic cells (DCs) are professional phagocytes that form a "cellular bridge" between the innate and adaptive immune system. In the lung, DCs are strategically located between the alveolar epithelium and the lung capillary system, where they are involved in sampling inhaled noninfectious and infectious particles, and in their processing and transportation into lung-draining lymph nodes to trigger immune responses or tolerance (1). The classical "myeloid" DC population of the lung was refined to consist of (at least) two subsets of DCs, immunophenotypically characterized as CD11b^{high} and major histocompatibility complex (MHC) Class II^{pos} DCs (CD11b^{pos} DCs), and CD103^{pos} DCs, which are characterized by their CD11b^{low}, MHC Class II^{pos}, and CD103^{pos} expression profiles. Both of these lung DC subsets were recently suggested to originate in noninflammatory and inflammatory monocyte precursors, respectively (2–4). More recent reports, however, suggest that in nonlymphoid organs such as the lung, CD103^{pos} DCs originate in bone marrow–derived pre-DCs, whereas CD11b^{pos} DCs are more heterogeneous (5).

DCs require both a fully functional state of differentiation and activation, and a tightly controlled pool size to contribute to the immunologic integrity of the lung (6, 7). Various DC subsets of extrapulmonary organ systems such as thymic and lymph-node DCs, as well as splenic DCs and epidermal Langerhans cells, were reported to exhibit significant radiosensitivity in response to whole-body irradiation and bone marrow transplantation (BMT) (8). For the lung, only limited information is available on the radiosensitivity of both major myeloid DC subsets. Irradiation/BMT therapeutic regimens are used in the treatment of certain hematologic malignancies, and are frequently accompanied by severe opportunistic lung infections, possibly attributable to the impact of these treatment protocols on pulmonary DC and macrophage subset homeostasis. A better understanding of the impact of these treatment regimens on DC homeostasis could lead to novel adjuvant/immune therapeutic interventions that would minimize the risk of developing opportunistic infections of the lung that often accompany irradiation/BMT protocols. We examined the effects of whole-body irradiation and subsequent BMT on lung CD11b^{pos} DC and CD103^{pos} DC subset pool sizes, and we determined detailed time response analyses of both CD11b^{pos} DC and CD103^{pos} DC turnover in the lung. To address this, we irradiated CD45.1 alloantigen-expressing recipient mice, and reconstituted their hematopoietic system with bone marrow cells from CD45.2 alloantigen-expressing donor mice. We then performed a detailed time response analysis of the depletion and repopulation characteristics, as well as turnover characteristics, of lung CD11b^{pos} DC and CD103^{pos} DC subsets, both at baseline and in response to bacterial pneumonia attributable to *Streptococcus pneumoniae*.

MATERIALS AND METHODS

Animals

Donor C57BL/6 mice were purchased from Charles River (Sulzfeld, Germany) and expressed the CD45.2 alloantigen on the cell surface of circulating leukocytes. Recipient B6.SJL-*Ptprc*^{a} mice (C57BL/6) expressing the CD45.1 alloantigen were purchased from Jackson Laboratories (Sacramento, CA), and were housed under conventional conditions and used in experiments at ages 7–16 weeks.

Reagents

The reagents used in this study are outlined in the online supplement.

Generation of Chimeric Mice

Chimeric mice were generated as previously described (9–11). For details, please see the online supplement. Animal experiments were approved by our local government authorities.

(*Received in original form June 1, 2010 and in final form December 6, 2010*)

Correspondence and requests for reprints should be addressed to Ulrich A. Maus, Ph.D., Department of Experimental Pneumology, Hannover School of Medicine, Hannover 30625, Germany. E-mail: Maus.Ulrich@mh-hannover.de

This article has an online supplement, which is accessible from this issue's table of contents at www.atsjournals.org

Am J Respir Cell Mol Biol Vol 45. pp 534–541, 2011
Originally Published in Press as DOI: 10.1165/rcmb.2010-0279OC on December 22, 2010
Internet address: www.atsjournals.org

Collection of Blood Leukocytes and Mononuclear Phagocyte Subsets from Lung Parenchymal Tissue and the Bronchoalveolar Space, and Determination of Their Turnover Kinetics

Mice were killed with an overdose of isoflurane (Baxter, Unterschleissheim, Germany) and their peripheral blood was immediately collected from the vena cava into EDTA-containing tubes, followed by the lysis of red blood cells with ammonium chloride buffer. Bone marrow engraftment in chimeric mice was assessed by a FACS-based immunophenotypic analysis of CD45 alloantigen expression profiles of peripheral blood leukocytes, as described in detail elsewhere (9, 12). Bronchoalveolar lavage (BAL) was performed as outlined in the online supplement. The analysis of lung macrophages was performed as described in detail elsewhere (7, 9), and is further outlined in the online supplement. We here define alveolar macrophages as those accessible by bronchoalveolar lavage, and lung macrophages as those retained in the lungs after lavage.

Immunophenotypic Analysis of CD45.1 and CD45.2 Cell Surface Antigen Expression of Lung Mononuclear Phagocyte Subsets

The turnover kinetics of lung CD11b^{pos} DCs and CD103^{pos} DCs, both of which express CD11c, were determined in lung parenchymal tissue of chimeric mice. The purification of CD11c-positive lung mononuclear phagocytes was performed using CD11c-labeled magnetic beads. The identification of CD11b^{pos} DCs and CD103^{pos} DCs was performed according to their forward-scatter/side-scatter characteristics and their low green autofluorescence properties, in conjunction with their CD11c^{pos}, CD11b^{high}, MHC Class II^{high}, CD103^{neg} (CD11b^{pos} DCs), CD11c^{pos}, CD11b^{low}, MHC Class II^{high}, and CD103^{pos} (CD103^{pos} DCs) immunophenotype, and their respective CD45.1 (recipient) or CD45.2 (donor) alloantigen expression profiles. The turnover kinetics of alveolar and lung macrophages were determined essentially as described elsewhere (9).

Analysis of Apoptosis and Necrosis

Irradiation-induced apoptosis and necrosis in lung mononuclear phagocyte subsets of chimeric mice were analyzed as outlined in the online supplement.

Infection Experiments with *S. pneumoniae*

In selected experiments, we determined the turnover kinetics of lung DCs and macrophages in response to acute inflammation triggered by "low-level" infection of mice with the prototype Gram-positive lung pathogen, *S. pneumoniae* (9, 11, 14–16). Chimeric CD45.1 mice were infected with *S. pneumoniae* on Day 10 or Day 35 after irradiation/BMT for the determination of infection-induced turnover of DCs and macrophages, respectively. For details, please see the online data supplement.

Statistical Analysis

All data are expressed as mean ± SEM. Significant differences between groups were analyzed by ANOVA, followed by the *post hoc* Dunnett test, using SPSS software (SPSS, Inc., Chicago, IL). Statistically significant differences between groups were assumed when $P < 0.05$.

RESULTS

Efficiency of Bone Marrow Engraftment in Chimeric CD45.1 Mice Assessed by CD45.2 Cell Surface Expression in Peripheral Blood Leukocytes

We evaluated the efficiency of bone marrow engraftment in irradiated CD45.1 recipient mice transplanted with CD45.2 bone marrow cells. Figure 1A illustrates the FACS-based immunophenotypic approach to discriminate between recipient (CD45.1) and donor-type (CD45.2) peripheral blood leukocytes (Figure 1A). Chimeric CD45.1 mice developed profound leukopenia as early as 3 days after treatment, which recovered to

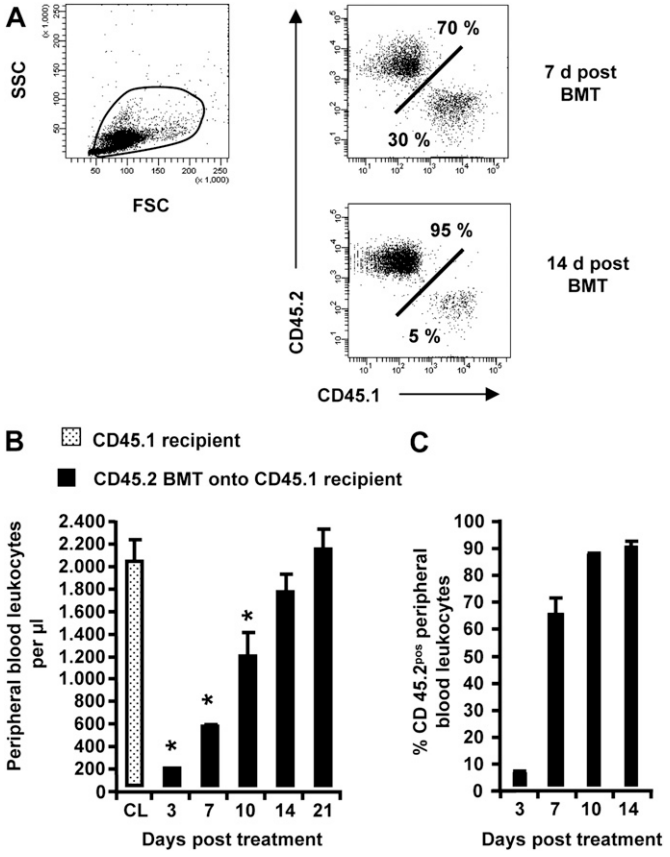

Figure 1. Immunophenotypic analysis of bone marrow engraftment in chimeric CD45.1 mice. CD45.1^{pos} recipients were irradiated and transplanted with bone marrow cells from CD45.2^{pos} donors (1×10^7 bone marrow cells/mouse). Peripheral blood was collected from control and chimeric CD45.1 mice. (*A–C*) Numbers of peripheral blood leukocytes were counted at different time points after irradiation and bone marrow transplantation (BMT), and were subsequently subjected to FACS analysis of CD45.1 versus CD45.2 alloantigen expression. The data are presented as mean ± SEM of $n \geq 4$ mice per time point. d, days; FSC, forward scatter; SSC, side scatter; CL, control. *Significant decrease ($P < 0.05$) compared with CD45.1 recipient mice (CL) at indicated time points.

baseline levels by Day 14 after treatment (Figure 1B). CD45.2 bone marrow engraftment reached nearly 70% by Day 7 after treatment, and reached an engraftment efficiency of 80–90% between Days 14–21 after treatment (Figure 1C). Consistent with previous reports (9), these data illustrate an exceedingly efficient engraftment process by which CD45.1^{pos} recipient-type peripheral blood leukocytes are replaced by CD45.2^{pos} donor-type cells in chimeric CD45.1 mice.

Effects of Irradiation and BMT on Pool Sizes and Turnover Kinetics of CD103^{pos} and CD11b^{pos} DCs in Lung Parenchymal Tissue of Chimeric CD45.1 Mice

We next aimed to determine the effects of irradiation and BMT on the numbers of CD103^{pos} DCs and CD11b^{pos} DCs in the lung tissue of chimeric CD45.1 mice. Figures 2A and 2B illustrate the gating strategy used to discriminate lung CD11b^{pos} DCs from CD103^{pos} DCs in purified CD11c^{pos} mononuclear phagocytes collected from the lung tissues of control mice and chimeric mice. Interestingly, we found a massive, nearly complete (>90%) depletion of CD103^{pos} DCs from the lung parenchymal tissue of mice undergoing irradiation/BMT, with lowest CD103^{pos} DC

counts observed on Day 3 (Figure 2C), with a repopulation toward baseline CD103^{pos} DC numbers by Days 21–28 after treatment. Consequently, the turnover rate of recipient versus donor-type CD45.2^{pos} lung CD103^{pos} DCs was found to be greater than 90% as early as Days 7–10 after irradiation (Figures 2D and 2E), demonstrating that lung CD103^{pos} DCs are extremely radiosensitive and are repopulated quickly. Lung CD11b^{pos} DCs were depleted to a lesser extent after irradiation/BMT in the lung tissue of chimeric CD45.1 mice (Figures 2F–2H), with the greatest depletion of lung CD11b^{pos} DCs at only approximately 60% by Day 5 after treatment, followed by repopulation of lung CD11b^{pos} DC numbers by Day 10. Relative to CD103^{pos} DCs, delayed turnover kinetics reached an 80–90% exchange of recipient versus donor-type lung CD11b^{pos} DCs by Days 21–28 after treatment (Figures 2F–2H). Notably, the turnover of CD103^{pos} DCs and CD11b^{pos} DCs in the lung-draining lymph nodes reached more than 80% for CD103^{pos} DCs and CD11b^{pos} DCs by Day 10 after irradiation and BMT, again demonstrating a brisk turnover of these two lung DC subsets (data not shown).

We also performed a comparative analysis of the turnover kinetics of alveolar and lung macrophages in the same mice under the same experimental conditions. Similar to the results for lung CD11b^{pos} DCs and CD103^{pos} DCs, irradiation/BMT also triggered a transient depletion of both alveolar macrophages (Figures 3A–3C) and lung macrophages (Figures 3D–3F) in the lungs of chimeric CD45.1 mice, but in contrast to lung CD11b^{pos} DCs and CD103^{pos} DCs, macrophages reached their maximal depletion on Day 21 after treatment, which is considerably delayed compared with lung CD103^{pos} DCs (peak of depletion, Day 3; Figure 2C) and lung CD11b^{pos} DCs (peak of depletion, Day 5; Figure 2F). This delay in macrophage depletion in response to irradiation/BMT was accompanied by a delayed reconstitution of both alveolar and lung macrophages, reaching an approximately 50% exchange of recipient versus donor-type macrophages by Day 42 after treatment (Figures 3C and 3F), and an overall turnover of approximately 90% by 10 weeks after treatment (Figures 3C and 3F), similar to the findings in previous reports (9, 12, 17).

Thus, our data show remarkably different replacement kinetics for the various mononuclear phagocyte subsets in the lungs of mice, with the fastest depletion and repopulation rates observed for lung CD103^{pos} DCs, followed by lung CD11b^{pos} DCs, and finally alveolar and lung macrophages on Days 21 and 42–70 after irradiation/BMT, respectively.

Pattern of Inducing Apoptosis and Necrosis in Chimeric Mice Subsequent to Irradiation and BMT

To determine the mechanism by which a regimen of irradiation/BMT triggers the brisk depletion of recipient-type DC subsets in the lungs of mice, we examined the induction of apoptosis and necrosis in CD45.1 cells. Figure 4 shows that the reduction of CD45.1 recipient-type lung DC numbers, observed as early as Days 3 and 5 after irradiation/BMT, was accompanied by a dramatically increased induction of apoptosis and necrosis in this phagocyte subset, with a peak of approximately 23% apoptotic and approximately 9% necrotic total lung DCs, respectively, observed only on Day 1 after treatment (Figures 4A and 4B), and declining toward lower values thereafter, just as the process of depletion subsided. A similar situation was evident for both CD45.1 recipient-type alveolar and lung macrophages, that is, a transient depletion in cell numbers was accompanied by a significantly increased induction of apoptosis and necrosis in these phagocytes, particularly at early time points (on Day 1 after treatment), when the depletion process was found to be initiated (Figures 4C–4F).

The Lung DC Turnover in Chimeric CD45.1 Mice Is Accelerated in Response to Low-Dose Infection with *S. pneumoniae*

Finally, we examined whether the pneumonia triggered by "low-dose" infection with *S. pneumoniae* would accelerate the repopulation and turnover kinetics of DC subsets in the lungs of chimeric CD45.1 mice. The infection of chimeric CD45.1 mice with *S. pneumoniae* (performed on Day 10 after irradiation/BMT) induced a strong recruitment of CD103^{pos} lung DCs within 7 days after infection (Figures 5A and 5B). Under these conditions, numbers of lung CD103^{pos} DCs were increased by 9-fold relative to control values (Figure 5A). Moreover, the numbers of lung CD11b^{pos} DCs were increased 14-fold on Day 2 after infection, relative to the numbers of CD11b^{pos} DCs observed before infection (Figure 5C). A complete turnover of recipient versus donor-type CD11b^{pos} DCs was evident on Days 1–2 after infection (Figure 5D).

We next analyzed the repopulation and turnover kinetics of alveolar and lung macrophages of chimeric CD45.1 mice. Mice were infected with a low dose of *S. pneumoniae* on Day 35 after irradiation/BMT, that is, when the pool of both alveolar and lung mononuclear phagocyte subsets was composed of 20–30% donor-type cells (CD45.2^{pos}) and 70–80% recipient-type cells (CD45.1^{pos}). We found that a low-dose infection of mice with *S. pneumoniae* triggered a 7-fold increased pool size of mononuclear phagocytes, both in the alveolar and lung parenchymal compartment relative to preinfection conditions, which remained elevated for 7 days after infection (Figures 5E and 5G). Consistent with recent reports (9), at 1–2 days after infection with *S. pneumoniae*, approximately 90% of BAL fluid mononuclear phagocytes and lung macrophages expressed the CD45.2 donor-type alloantigen, representing newly recruited cells (Figures 5F and 5H). These data clearly demonstrate that the infection of chimeric CD45.1 mice with *S. pneumoniae* triggers a rapid recruitment of immune cells and thus a rapid replacement of resident CD45.1^{pos} recipient-type cells by newly recruited CD45.2^{pos} donor-type cells.

DISCUSSION

The main goal of our study was to determine the impact of whole-body irradiation and BMT on the repopulation profile and turnover characteristics of lung DC subsets, compared with alveolar and lung macrophages under baseline and inflammatory conditions, using *S. pneumoniae* as an inflammatory stimulus. To the best of our knowledge, we show for the first time that irradiation/BMT triggers a rapid, greater than 90% depletion of CD103^{pos} DCs from the lung parenchymal tissue of mice by Day 3 after irradiation, whereas CD11b^{pos} DCs are only depleted by approximately 50–60% on Day 5 after treatment. In contrast to these data, alveolar and lung macrophages are depleted much later, by Day 21 after treatment, reaching a maximal depletion of only 50–60%. Moreover, we observed a differentially regulated repopulation of lung tissue within the respective lung DC and macrophage subsets. Whereas lung CD11b^{pos} DCs and lung CD103^{pos} DCs reached their original pool size by Days 10 and 21 after treatment, respectively, the repopulation of alveolar and lung macrophages reached baseline pool sizes on Days 42 and 70 after treatment, respectively. Furthermore, the infection of chimeric mice with low levels of *S. pneumoniae* triggered a brisk acceleration of the repopulation of all myeloid-derived DC and macrophage subsets in the lung. Altogether, our study provides a comprehensive analysis of the effects of irradiation/BMT on the depletion and repopulation and turnover kinetics of the major myeloid-derived lung DC and macrophage subsets, under both

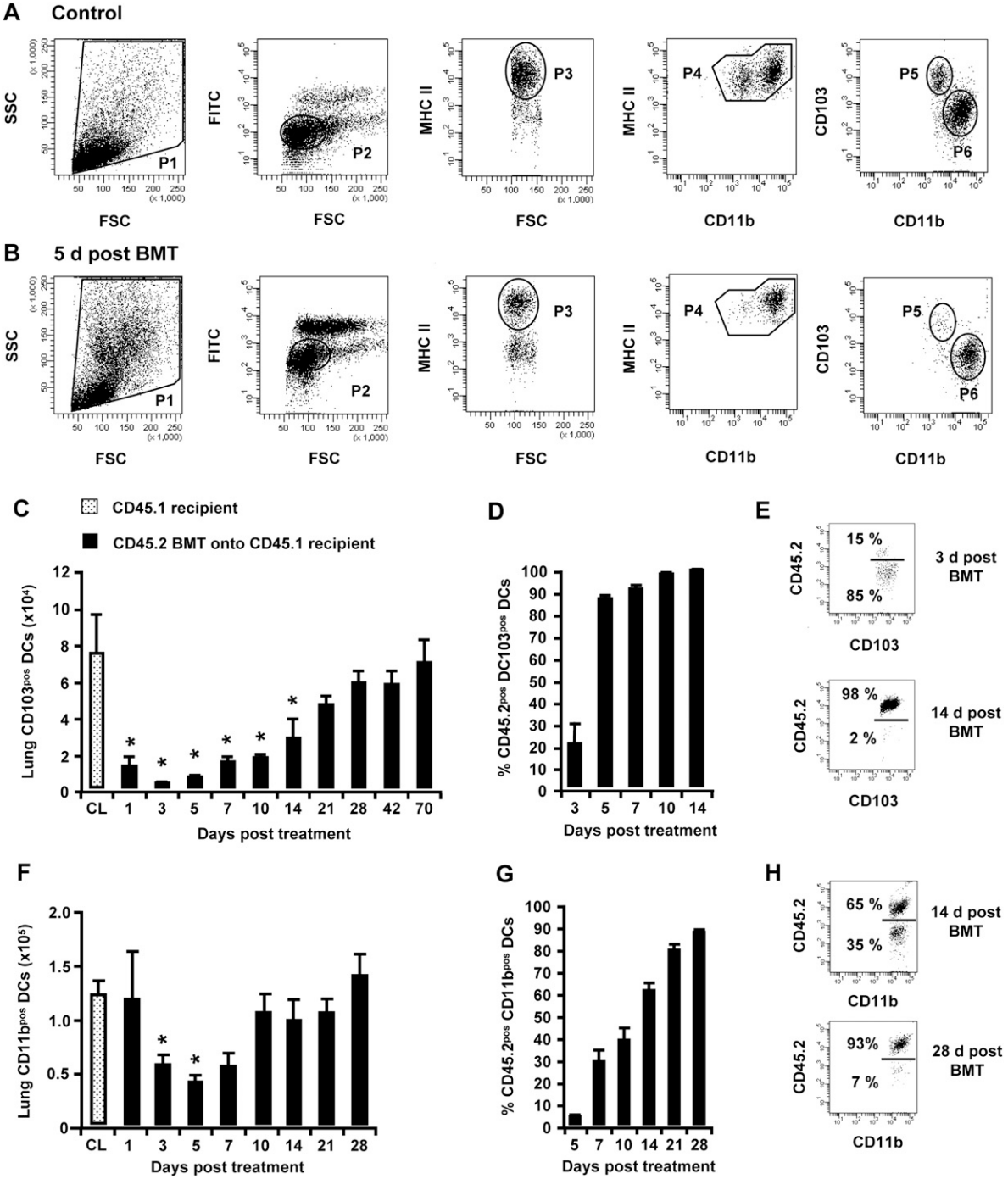

Figure 2. Turnover kinetics of lung CD103^{pos} dendritic cells (DCs) and lung CD11b^{pos} DCs in chimeric CD45.1 mice. Lungs of control mice and chimeric CD45.1 mice were initially subjected to bronchoalveolar lavage (BAL) to remove alveolar macrophages, followed by the enrichment of lung mononuclear phagocyte subsets (including CD11b^{pos} DCs and CD103^{pos} DCs), using CD11c-labeled magnetic beads. (*A*, *B*, *E*, and *H*) Representative FACS analyses of the baseline turnover of lung CD103^{pos} DCs and lung CD11b^{pos} DCs, gated according to their FSC versus SSC characteristics (P1), followed by hierarchical subgating according to their FSC versus low green autofluorescence (P2) and CD11c cell surface expression. Lung DC subsets were further subgated according to FSC versus major histocompatibility complex (MHC) Class II (P3), CD11b versus MHC Class II (P4), and CD11b versus CD103 (P5, CD103^{pos} DCs; P6, CD11b^{pos} DCs), followed by analyses of their CD45.1 or CD45.2 cell-surface expression (*E* and *H*). We also performed the quantification of total numbers of (*C*) CD103^{pos} DCs and (*F*) CD11b^{pos} DCs purified from lung parenchymal tissue digests. We further performed the quantification of (*C* and *D*) CD45.2^{pos} donor-type lung CD103^{pos} DCs and (*F* and *G*) lung CD11b^{pos} DCs. The data are presented as mean ± SEM of $n \geq 4$–12 mice per time point. *Significant decrease ($P < 0.05$) compared with CD45.1 recipient mice (CL) at the indicated time points.

baseline and infection conditions. This information could be particularly important in the development of adjuvant immune enhancement strategies to overcome the immunosuppression of whole-body–irradiated BMT recipients.

Our report contains several novel aspects. First, to the best of our knowledge, we are the first to provide a detailed subset-specific analysis of the depletion and repopulation and turnover kinetics of both CD103^{pos} and CD11b^{pos} DC subsets in a chimeric

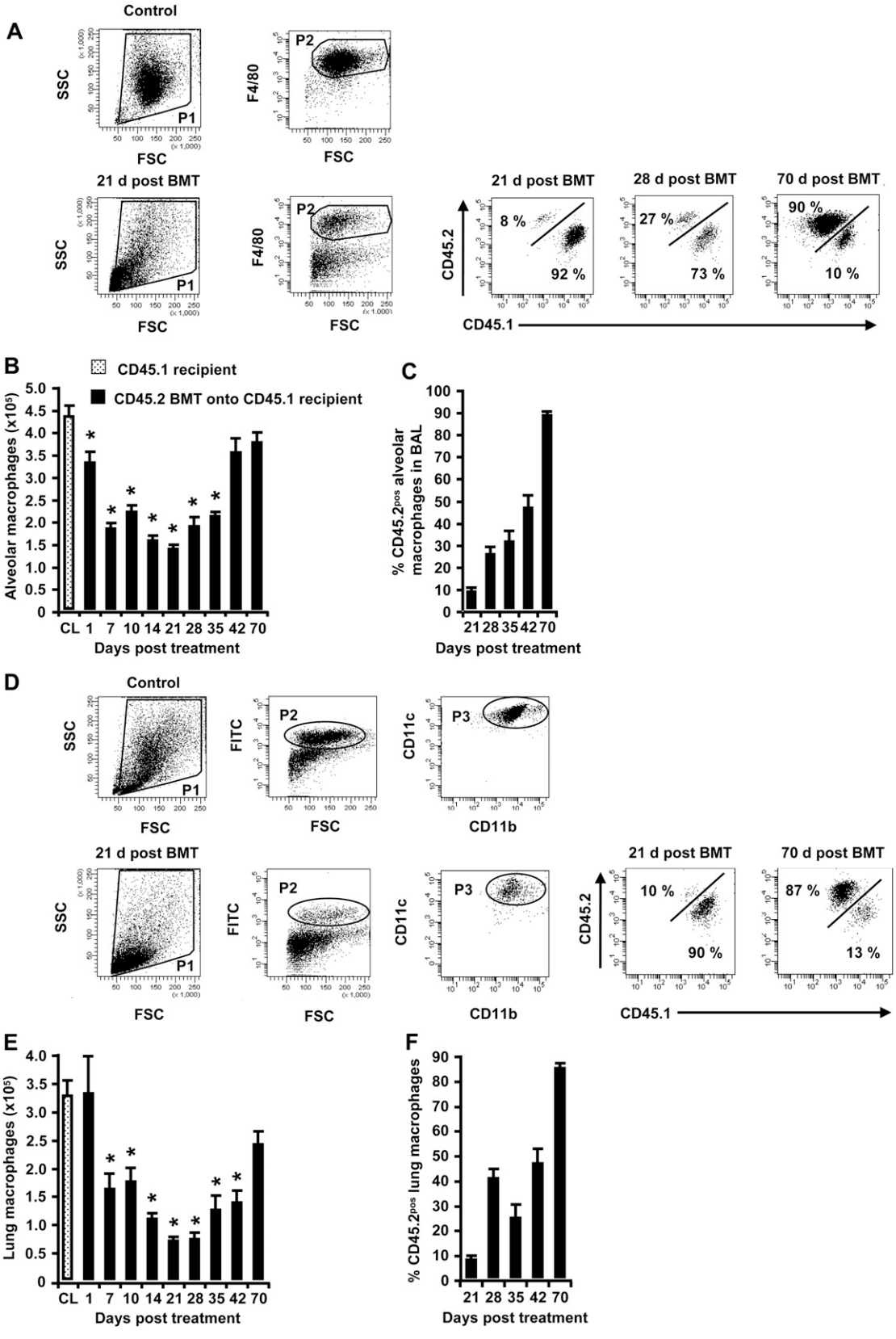

Figure 3. Depletion and repopulation and turnover kinetics of alveolar macrophages and lung macrophages in chimeric CD45.1 mice. (*A* and *C*) Representative FACS analysis of the baseline turnover of alveolar macrophages, gated according to their FSC versus SSC characteristics (P1), followed by hierarchical subgating according to their FSC versus F4/80 antigen expression characteristics (P2), followed by a determination of their turnover profiles according to CD45.2 versus CD45.1 alloantigen expression. (*B* and *C*) At the indicated time points, chimeric CD45.1 mice were killed, and the numbers and CD45 phenotypes of alveolar macrophages were determined in whole-lung washes. (*D–F*) Lung macrophages were collected from the lung tissue of chimeric CD45.1 mice at different time points after irradiation/BMT, and the quantification of total numbers of green autofluorescent/CD11c^{pos} cells was performed according to the FACS-based identification of CD45.2^{pos} donor-type cells. Data are presented as mean ± SEM of $n = 4$–12 mice per time point. *Significant decrease ($P < 0.05$) compared with CD45.1 recipient mice (CL).

irradiation/BMT murine model system. Second, we demonstrate that CD103^{pos} DCs in the lung are more sensitive than CD11b^{pos} DCs and lung macrophages to irradiation, resulting in an overall transient depletion of more than 90% in chimeric mice. Third, we show a rapid repopulation of the lungs with CD103^{pos} DC and CD11b^{pos} DC subsets subsequent to irradiation/BMT within 10 days (CD11b^{pos} DCs) and 21 days (CD103^{pos} DCs) after treatment, respectively, whereas alveolar and lung macrophages exhibit a more delayed depletion and repopulation, by Days 21 and 70 after treatment, respectively. Finally, we provide evidence that

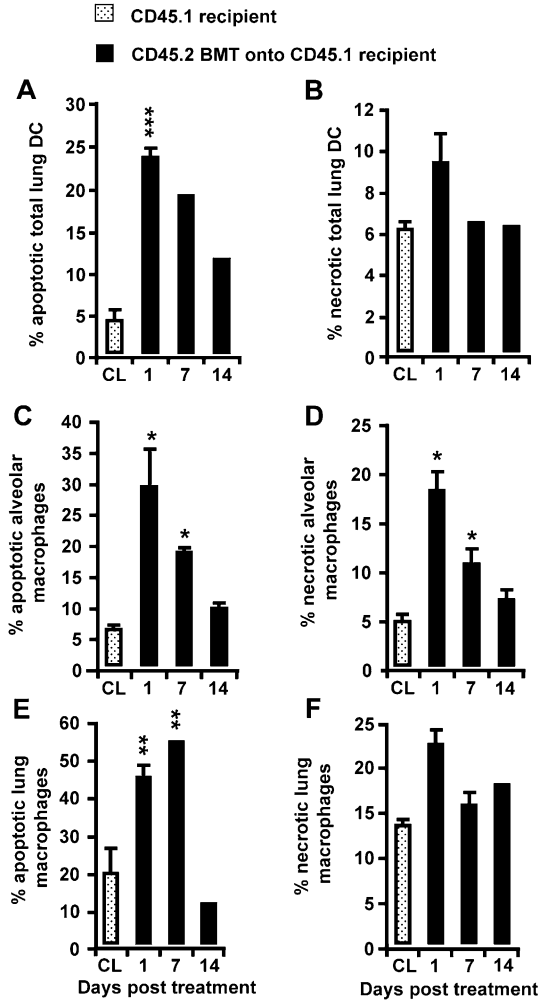

Figure 4. Determination of apoptosis and necrosis induced in CD45.1 recipient-type lung DCs and alveolar and lung macrophages of chimeric CD45.1 mice. Chimeric CD45.1 mice were subjected to BAL, followed by lung tissue digestion, as outlined in MATERIALS AND METHODS. Subsequently, total lung DCs (*A* and *B*) and alveolar macrophages (*C* and *D*), as well as lung macrophages (*E* and *F*), were stained with annexin V and 7-Aminoactinomycin D (7-AAD) for a FACS analysis of the induction of apoptosis and necrosis, as indicated. Because of the low numbers of lung DC subsets observed on Days 1–14 after irradiation/BMT, the induction of apoptosis and necrosis shown in *A* and *B* was analyzed in total lung DCs. Data are presented as mean ± SEM of at least 3–4 mice per time point. A significant increase (*$P < 0.05$, **$P < 0.01$) was evident, compared with CD45.1 recipient mice (CL).

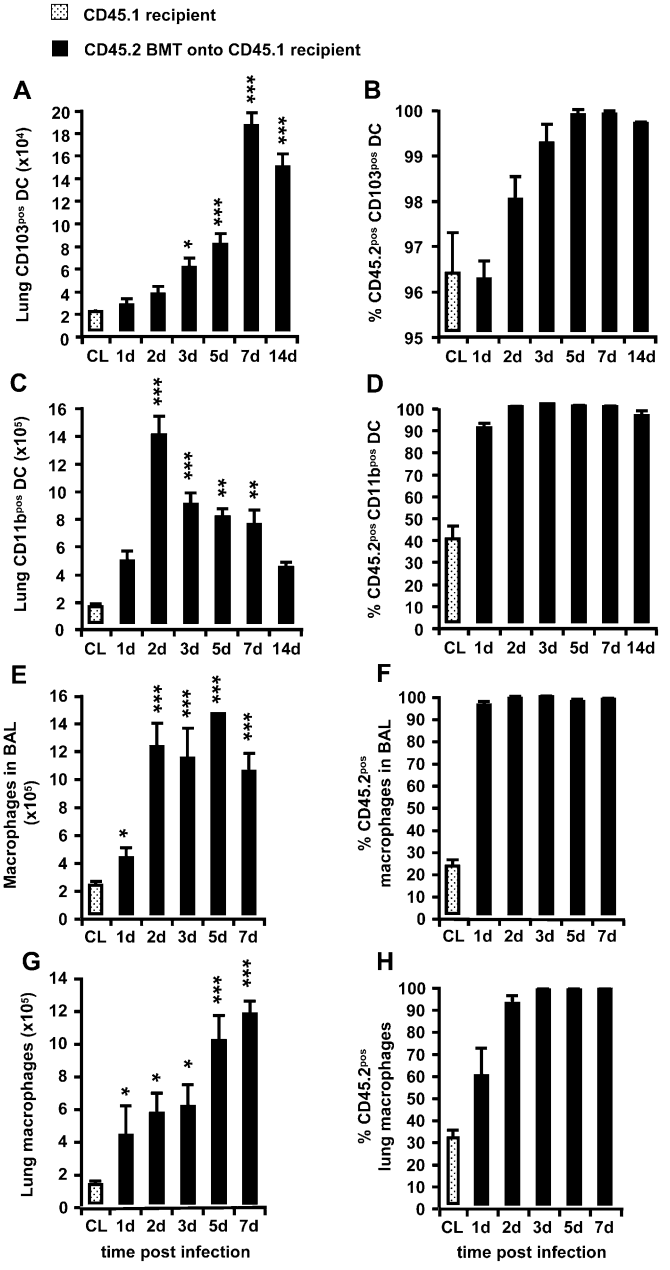

Figure 5. Turnover kinetics of lung CD103^{pos} DCs and lung CD11b^{pos} DCs versus macrophages in chimeric CD45.1 mice after low-dose infection with *S. pneumoniae*. Chimeric CD45.1 mice were infected with *S. pneumoniae* on Days 10 or 35 after irradiation/BMT, followed by a determination of repopulation and turnover profiles of the various mononuclear phagocyte subsets at the indicated time points. (*A–D*) Total numbers and percentages of CD45.2^{pos} CD103^{pos} DCs (*A* and *B*) and CD11b^{pos} DCs (*C* and *D*). (*E–H*) Total numbers and percentages of CD45.2^{pos} alveolar macrophages (*E* and *F*) and lung macrophages (*G* and *H*). The data are presented as the mean ± SEM of $n = 3$–9 mice per time point. A significant increase (*$P < 0.05$, **$P < 0.01$, and ***$P < 0.001$) was evident, compared with CL.

all myeloid-derived phagocyte subsets examined in the present study, including lung CD103^{pos} DCs, lung CD11b^{pos} DCs, and alveolar and lung macrophages, are eliminated from the lung parenchymal and bronchoalveolar compartment subsequent to irradiation by apoptosis-mediated and necrosis-mediated processes. Previous investigators observed a decline in rat airway MHC Class II^{pos} cells shortly after irradiation/BMT, but they thought this decline was attributable to the emigration of mature DCs to regional lymph nodes (18). Our data indicate, however, that elevated levels of apoptosis and necrosis occur in all lung mononuclear phagocyte subsets after irradiation/BMT, indicating that this is the major mechanism underlying the process of depletion. Furthermore, we observed that the draining lymph nodes of the lungs of chimeric mice also contain reduced numbers of CD103^{pos} DCs and CD11b^{pos} DCs (data not shown).

One major difficulty when comparing the published turnover kinetics of mononuclear phagocyte subsets in the lungs or in extrapulmonary organ systems is related to the different experimental protocols used in the various reported studies. Here, we used a linear accelerator (also used in the therapeutic whole-body irradiation of BMT recipients) and an irradiation/BMT protocol, resulting in an overall engraftment efficacy of greater than 90%.

In a recent study by Ginhoux and colleagues, where parabiosis and separation experiments were performed in BL/6 mice and BL/6 CD45.1^{pos} mice, relatively short half-lives were also reported for both lung DC subsets (5). However, comparing these two model systems is difficult, particularly because of the limited clinical relevance of parabiosis model systems. Another study using a different irradiation protocol reported that numbers of macrophages in the alveolar compartment were restored within 30 days after irradiation (17), whereas in our study, the time needed to restore numbers of macrophages in the alveolar compartment and lung parenchymal tissue comprised approximately 42–70 days. These data clearly indicate that different experimental protocols may affect the comparative analyses of DCs and of macrophage turnover kinetics between different studies.

The origin of various lung DC subsets in the bone marrow and their developmental stages are still subject to ongoing debate. In this regard, a bone marrow precursor of macrophages and DCs, termed the macrophage and DC progenitor, and a common DC precursor were proposed to have the potential to differentiate into monocytes, macrophages, and different DC subsets (19, 20). Moreover, recent data indicate that two distinct murine blood monocyte populations can serve as DC precursors (21). Given the nearly complete depletion of CD103^{pos} DCs in lung parenchymal tissue reported in this study, and furthermore, given that in the present chimeric murine model, bone marrow cells from normal BL/6 mice (characterized by their CD45.2 alloantigen expression) were used as donor bone marrow, the present irradiation and transplantation protocol may also prove useful in identifying candidate molecules that may regulate the developmental pathways of progenitor cells giving rise to CD103^{pos} lung DCs, as already proven for CCR2 (22).

The repopulation and turnover kinetics of lung CD11b^{pos} DCs and CD103^{pos} DCs upon infection with *S. pneumoniae* constitute another aspect of the present report. We infected mice with a clinical isolate of serotype 19 *S. pneumoniae*, using a "low-level" inoculum size of 10^6 CFUs/mouse. This inoculum size is known to cause mild lobar pneumonia in mice, without causing severe lung tissue destruction or invasive disease progression (15). Despite this relatively weak bacterial challenge, we found that the rapid depletion of DC subsets was followed by a large recruitment of donor-type CD11b^{pos} DCs and CD103^{pos} DCs. These data illustrate that the lung host defense machinery responds to infection not only with a transient increase of lung macrophage pool size, as recently reported (9, 12), but also with an increased recruitment of lung CD11b^{pos} DCs and CD103^{pos} DCs. Interestingly, this transient "overshooting" mobilization of donor-type DCs was particularly evident in the later phase of pneumococcal pneumonia, when both the process of bacterial pathogen elimination and the recruitment of alveolar neutrophils had already returned to baseline (data not shown). However, the relevance of an increased lung DC pool size to the resolution/repair process in pneumococcal pneumonia is not yet clear, as opposed to the relevance of lung macrophages, which we previously showed to play a prominent role in the resolution/repair process subsequent to lung infection with *S. pneumoniae*, in terms of regaining lung homeostasis (13, 16, 23), However, we speculate that lung DC subsets, which are located beneath the alveolar epithelial barrier, may be involved in sensing apoptotic/necrotic neutrophils or responding to inflammatory mediators, thereby possibly contributing to host-derived inflammatory cytokine/chemokine responses subsequent to infection.

In conclusion, this study, to the best of our knowledge, is the first to provide a detailed comparative analysis of the turnover kinetics of lung DC and macrophage subsets under noninfectious conditions, as well as in response to infection with *S. pneumoniae*. We show that under noninfectious conditions, CD103^{pos} lung DCs were almost completely depleted from lung tissue after irradiation/BMT, indicating their strong radiosensitivity. Moreover, the turnover of lung CD103^{pos} DCs was clearly accelerated compared with lung CD11b^{pos} DCs, and both DC subsets exhibited a strongly accelerated turnover profile relative to alveolar and lung macrophages. Moreover, we demonstrated a brisk repopulation and turnover of all mononuclear phagocyte subsets after low-dose infection with *S. pneumoniae*. We believe that our newly provided information on the irradiation-induced effects of baseline and inflammation-induced lung DC and macrophage turnover profiles will be of major clinical importance in the development of immune-supportive therapeutic or prophylactic treatment regimens, to lower the risk of both bacterial and viral infections in irradiated BMT recipients.

Author Disclosure: None of the authors have a financial relationship with a commercial entity that has an interest in the subject of this manuscript.

References

1. Holt PG, Strickland DH, Wikstrom ME, Jahnsen FL. Regulation of immunological homeostasis in the respiratory tract. *Nat Rev Immunol* 2008;8:142–152.
2. Sung SS, Fu SM, Rose CE Jr, Gaskin F, Ju ST, Beaty SR. A major lung CD103 (alphaE)–beta7 integrin-positive epithelial dendritic cell population expressing Langerin and tight junction proteins. *J Immunol* 2006;176:2161–2172.
3. Beaty SR, Rose CE Jr, Sung SS. Diverse and potent chemokine production by lung CD11b high dendritic cells in homeostasis and in allergic lung inflammation. *J Immunol* 2007;178:1882–1895.
4. del Rio ML, Rodriguez-Barbosa JI, Bolter J, Ballmaier M, Dittrich-Breiholz O, Kracht M, Jung S, Forster R. CX3CR1+ c-kit$^+$ bone marrow cells give rise to CD103$^+$ and CD103$^-$ dendritic cells with distinct functional properties. *J Immunol* 2008;181:6178–6188.
5. Ginhoux F, Liu K, Helft J, Bogunovic M, Greter M, Hashimoto D, Price J, Yin N, Bromberg J, Lira SA, *et al.* The origin and development of nonlymphoid tissue CD103$^+$ DCs. *J Exp Med* 2009;206:3115–3130.
6. von Wulffen W, Steinmueller M, Herold S, Marsh LM, Bulau P, Seeger W, Welte T, Lohmeyer J, Maus UA. Lung dendritic cells elicited by FMS-like tyrosine 3–kinase ligand amplify the lung inflammatory response to lipopolysaccharide. *Am J Respir Crit Care Med* 2007;176:892–901.
7. Winter C, Taut K, Langer F, Mack M, Briles DE, Paton JC, Maus R, Srivastava M, Welte T, Maus UA. FMS-like tyrosine kinase 3 ligand aggravates the lung inflammatory response to *Streptococcus pneumoniae* infection in mice: role of dendritic cells. *J Immunol* 2007;179:3099–3108.
8. Merad M, Manz MG. Dendritic cell homeostasis. *Blood* 2009;113:3418–3427.
9. Taut K, Winter C, Briles DE, Paton JC, Christman JW, Maus R, Baumann R, Welte T, Maus UA. Macrophage turnover kinetics in the lungs of mice infected with *Streptococcus pneumoniae. Am J Respir Cell Mol Biol* 2008;38:105–113.
10. Maus UA, Waelsch K, Kuziel WA, Delbeck T, Mack M, Blackwell TS, Christman JW, Schlondorff D, Seeger W, Lohmeyer J. Monocytes are potent facilitators of alveolar neutrophil emigration during lung inflammation: role of the CCL2–CCR2 axis. *J Immunol* 2003;170:3273–3278.
11. Herbold W, Maus R, Hahn I, Ding N, Srivastava M, Christman JW, Mack M, Reutershan J, Briles DE, Paton JC, *et al.* Importance of CXC chemokine receptor 2 in alveolar neutrophil and exudate macrophage recruitment in response to pneumococcal lung infection. *Infect Immun* 2010;78:2620–2630.
12. Maus UA, Janzen S, Wall G, Srivastava M, Blackwell TS, Christman JW, Seeger W, Welte T, Lohmeyer J. Resident alveolar macrophages are replaced by recruited monocytes in response to endotoxin-induced lung inflammation. *Am J Respir Cell Mol Biol* 2006;35:227–235.
13. Winter C, Taut K, Srivastava M, Langer F, Mack M, Briles DE, Paton JC, Maus R, Welte T, Gunn MD, *et al.* Lung-specific overexpression of CC chemokine ligand (CCL) 2 enhances the host defense to *Streptococcus pneumoniae* infection in mice: role of the CCL2–CCR2 axis. *J Immunol* 2007;178:5828–5838.

14. Henken S, Bohling J, Martens-Lobenhoffer J, Paton JC, Ogunniyi AD, Briles DE, Salisbury VC, Wedekind D, Bode-Boger SM, Welsh T, *et al.* Efficacy profiles of daptomycin for treatment of invasive and noninvasive pulmonary infections with *Streptococcus pneumoniae*. *Antimicrob Agents Chemother* 2010;54:707–717.
15. Briles DE, Crain MJ, Gray BM, Forman C, Yother J. Strong association between capsular type and virulence for mice among human isolates of *Streptococcus pneumoniae*. *Infect Immun* 1992;60:111–116.
16. Maus UA, Backi M, Winter C, Srivastava M, Schwarz MK, Ruckle T, Paton JC, Briles D, Mack M, Welte T, *et al.* Importance of phosphoinositide 3–kinase gamma in the host defense against pneumococcal infection. *Am J Respir Crit Care Med* 2007;175:958–966.
17. Matute-Bello G, Lee JS, Frevert CW, Liles WC, Sutlief S, Ballman K, Wong V, Selk A, Martin TR. Optimal timing to repopulation of resident alveolar macrophages with donor cells following total body irradiation and bone marrow transplantation in mice. *J Immunol Methods* 2004;292:25–34.
18. Holt PG, Stumbles PA. Characterization of dendritic cell populations in the respiratory tract. *J Aerosol Med* 2000;13:361–367.
19. del Rio ML, Bernhardt G, Rodriguez-Barbosa JI, Forster R. Development and functional specialization of CD103$^+$ dendritic cells. *Immunol Rev* 2010;234:268–281.
20. Liu K, Nussenzweig MC. Origin and development of dendritic cells. *Immunol Rev* 2010;234:45–54.
21. Jakubzick C, Tacke F, Ginhoux F, Wagers AJ, van Rooijen N, Mack M, Merad M, Randolph GJ. Blood monocyte subsets differentially give rise to CD103$^+$ and CD103$^-$ pulmonary dendritic cell populations. *J Immunol* 2008;180:3019–3027.
22. Dominguez PM, Ardavin C. Differentiation and function of mouse monocyte–derived dendritic cells in steady state and inflammation. *Immunol Rev* 2010;234:90–104.
23. Winter C, Herbold W, Maus R, Langer F, Briles DE, Paton JC, Welte T, Maus UA. Important role for CC chemokine ligand 2–dependent lung mononuclear phagocyte recruitment to inhibit sepsis in mice infected with *Streptococcus pneumoniae*. *J Immunol* 2009;182:4931–4937.